

Shot-noise limited detection sensitivity in multiplex CARS microscopy

Michiel Müller^a, Juleon M. Schins^b, G.W.H. Wurpel^a

^aSwammerdam Institute for Life Sciences, University of Amsterdam, P.O. Box 94062, 1090 GB Amsterdam, The Netherlands

^bCurrent address: Radiation Chemistry Department, Interfaculty Reactor Institute, Delft University of Technology, Mekelweg 15, 2629 JB Delft, The Netherlands

ABSTRACT

In multiplex CARS microscopy the generated anti-Stokes signal is generated and detected simultaneously over a significant part of the vibrational spectrum. The signal-to-noise ratio of the thus detected spectra is limited only by shot-noise. This principle is demonstrated using a dilution series of 2-propanol in water. It is derived theoretically and shown experimentally that for low solute concentrations - in contrast to methods that suppress the non-resonant background - the CARS signal strength from a particular vibrational mode depends linearly on its concentration. Furthermore, excellent agreement is shown between the experimental data and fits to the theory. It is shown that this approach permits rapid (20 ms acquisition) detection of a single lipid mono-layer, with sufficient signal-to-noise to determine the order parameter for the acyl chain packing. Also it is demonstrated that this detection scheme provides an absolute measure of the solute concentration.

Keywords: Coherent anti-Stokes Raman scattering, microscopy, non-linear optics, lipid phase behaviour, lipid mono- and bilayers

1. INTRODUCTION

Vibrational spectroscopy probes the intra- and intermolecular vibrational structure of molecules and molecular assemblies, providing detailed information on both the chemistry and physics of the sample. Unique to this area of spectroscopy is that many of the spectral features remain resolvable even at room temperature and in complex samples such as live cells [1] and that it does not require any form of labeling. Spatially resolved spectroscopic information can be obtained by combining the vibrational spectroscopic techniques (e.g. infrared absorption and spontaneous Raman scattering) with high resolution microscopy. Infrared absorption can be used only at moderate spatial resolution because of the long wavelengths ($> 3 \mu\text{m}$) involved. On the other hand, the signal from spontaneous Raman scattering is weak and readily overwhelmed by the natural luminescence from the sample. A combination of conditions which is often prohibitive for application to high resolution microscopy.

Recently coherent anti-Stokes Raman Scattering (CARS) has been applied to high resolution optical microscopy [2-9]. This non-linear optical technique provides signal levels which are many orders of magnitude (> 4) stronger than attainable for spontaneous Raman scattering. In this third-order non-linear optical process two laser fields - denoted by *Pump* and *Stokes* (with frequency ω_p and ω_s respectively) - are mixed in the sample to generate an *anti-Stokes* signal at frequency $\omega_{as} = 2\omega_p - \omega_s$. The signal propagates coherently and is of shorter wavelength than all the input fields making it readily detectable.

A particularly attractive mode of operation is multiplex CARS microscopy [6]. Here a broad-band (femtosecond) *Stokes* laser is used in combination with a narrow-band (picosecond) *Pump* laser, concurrently generating an *anti-Stokes* signal over a significant part of the vibrational spectrum. The spectral resolution is determined by the *Pump* laser. Chemical identification or characterisation of the physical state of the sample generally requires the analysis of spectral line shapes, relative peak heights of different vibrational features, etc.. Resolving these features in single-point CARS (i.e. with both a narrow-band *Pump* and *Stokes* laser) is limited by fluctuations in pulse energy, pulse width and timing jitter. In multiplex CARS, on the other hand, the spectral signal-to-noise ratio (SNR) is shot-noise limited, permitting both detailed analysis of the spectral features and retrieving signals from species present at low concentration only.

In this paper we will demonstrate the shot-noise limited detection capability of multiplex CARS microscopy. After a theoretical introduction to analyse the dependence of the CARS signal strength with the solute concentration, we demonstrate the principle on a dilution series of 2-propanol in water. It is shown that for low concentrations the CARS signal strength follows the expected linear dependence on the concentration. We also show the correspondence between the measured spontaneous Raman signal and the measured and calculated multiplex CARS spectrum. As a further demonstration of the detection sensitivity of this approach we show detailed CARS spectra of a single lipid mono- and bilayer. Finally we discuss the potential of this approach and compare it to other modes of detection in CARS microscopy.

2. MULTIPLEX COHERENT ANTI-STOKES SCATTERING - THEORY

In the frequency domain, the third-order polarisation induced by two laser fields *Pump* ($E_p(\omega_p)$) and *Stokes* ($E_s(\omega_s)$) can generally be written as a triple integral over all frequencies involved. In the case of multiplex CARS the field $E_s(\omega_s)$ is provided by a spectrally broad laser, thus ensuring a large spectral band, and the field $E_p(\omega_p)$ by a spectrally narrow laser, defining the spectral resolution. The analytical expressions can be kept simple by writing the narrow laser field as a delta function:

$$E_p(\omega_p) \approx E_p \delta(\omega - \omega_p) \quad (1)$$

In this approximation the third-order polarisation $P^{(3)}(\omega_{AS})$ depends —for a unique and linear polarisation direction— on the electric fields as follows:

$$P^{(3)}(\omega_{AS}) \propto N \cdot E_p^2 E_s^* (\omega_s) \chi_{1111}^{(3)}(-\omega_{AS}; \omega_p, -\omega_s, \omega_p) \quad (2)$$

where $\chi_{1111}^{(3)}(-\omega_{AS}; \omega_p, -\omega_s, \omega_p)$ is the third order susceptibility, N the molarity (number of moles per unit volume) and where $\omega_s = 2\omega_p - \omega_{AS}$ is assumed implicitly in what follows. The lineshape of the CARS signal follows from

$$S(\omega_{AS}) = |P^{(3)}(\omega_{AS})|^2 \propto |E_s(\omega_s)|^2 |\chi_{1111}^{(3)}(-\omega_{AS}; \omega_p, -\omega_s, \omega_p)|^2 \quad (3)$$

Far away from one-photon resonances, this susceptibility can in general be written as a sum of two terms (omitting obvious subscripts and arguments)

$$\chi_{1111}^{(3)}(\omega) = \chi_{NR} + \chi_r(\omega) \quad (4)$$

where the non-resonant term (χ_{NR}) is independent of frequency and real, while the resonant term (χ_R) is complex and depends on frequency as follows:

$$\chi^{(res)}(\omega_{AS}) = \sum_j \frac{R_j}{\omega_{AS} - \omega_p - \Omega_j - i\Gamma_j} \quad (5)$$

Here, the sum runs over all involved vibrational resonances, each of them characterised by three parameters: eigenfrequency Ω_j , oscillator strength R_j , and linewidth Γ_j .

Low concentration signal. Next we consider the multiplex CARS signal from one molecular species of interest within a host material of another molecular species. More specifically, in our dilution experiments described below, 2-propanol molecules are detected at increasing dilution levels in water. The total multiplex CARS signal emitted in the forward direction is detected. The contributions to this signal can be grouped into a non-resonant term, a cross term and a resonant term:

$$\begin{aligned} S_{CARS}^{total} &\propto \left| N_w \chi_{NR,w} + N_{prop} \chi_{NR,prop} + N_{prop} \chi_{R,prop} \right|^2 = \\ &= \left| N_w \chi_{NR,w} + N_{prop} \chi_{NR,prop} \right|^2 + 2 \left(N_w \chi_{NR,w} + N_{prop} \chi_{NR,prop} \right) \text{Re} \left\{ N_{prop} \chi_{R,prop} \right\} + \left| N_{prop} \chi_{R,prop} \right|^2 \end{aligned} \quad (6)$$

where N_w and N_{prop} are the molarities of water and propanol respectively. For the sake of simplicity, the frequency dependencies have been omitted, as well as the broadband laser lineshape. In the case of low propanol concentration ($N_{prop} \ll N_w$) the resonant term becomes negligible with respect to the cross term, and the total signal can be approximated by

$$S_{CARS}^{total} \approx \left(N_w \chi_{NR,w} \right)^2 + 2 N_w N_{prop} \chi_{NR,w} \text{Re} \left\{ \chi_{R,prop} \right\} \quad (7)$$

Thus, at low solute concentrations, the CARS signal strength from the solute depends linearly on its concentration.

Raman and CARS. In this section we briefly review the theoretical expressions for the line shapes of spontaneous Raman scattering and CARS measurements. For the sake of simplicity, we shall consider a three-level system, where $|g\rangle$ represents the electro-vibrational ground state, $|v\rangle$ the first excited vibrational state in the electronic ground state, and $|e\rangle$ the lowest excited electronic state. The pertinent transition dipole moments are written as $\vec{\mu}_{ab}^j = -e \langle a | \vec{r}_j | b \rangle$, where r_j is the j-th component of the electron's position. The corresponding line widths are denoted by Γ_{ab} , and the energy differences by $\omega_{ab} = (E_a - E_b)/\hbar$.

In the absence of proper dephasing (due, for example, to collisions) the line shape for the CARS process can be written as (see e.g. [10, 11]):

$$S_{CARS} = \left| \frac{\rho_{gg}^{(0)}}{\omega_{vg} - (\omega_p - \omega_s) - i\Gamma_{vg}} \cdot \frac{(\vec{\epsilon}_p \cdot \vec{\mu}_{ge})(\vec{\epsilon}_s^* \cdot \vec{\mu}_{ev})}{\omega_{eg} - \omega_p - i\Gamma_{eg}} \cdot \frac{(\vec{\epsilon}_p \cdot \vec{\mu}_{ve})(\vec{\epsilon}_{AS} \cdot \vec{\mu}_{eg})}{\omega_{eg} - \omega_{AS} - i\Gamma_{eg}} \right|^2 \quad (8)$$

where $\rho_{gg}^{(0)}$ denotes the initial ground state density matrix element, $\vec{\epsilon}_p$, $\vec{\epsilon}_s$ indicate the unit vectors of the laser fields, and $\vec{\epsilon}_{AS}$ that of the analyser in the signal channel. The spontaneous Raman scattering line shape, on the other hand, is given by [11]:

$$S_{Raman} = i \frac{\rho_{gg}^{(0)}}{\omega_{vg} - (\omega_p - \omega_s) - i\Gamma_{vg}} \cdot \frac{(\vec{\epsilon}_p \cdot \vec{\mu}_{ge})(\vec{\epsilon}_s^* \cdot \vec{\mu}_{ev})}{\omega_{eg} - \omega_p - i\Gamma_{eg}} \cdot \frac{(\vec{\epsilon}_s \cdot \vec{\mu}_{ve})(\vec{\epsilon}_p^* \cdot \vec{\mu}_{eg})}{\omega_{ve} + \omega_s - i\Gamma_{ve}} + c.c. \quad (9)$$

For $\Gamma_{ve} \approx \Gamma_{eg}$ it follows, using the resonance condition $\omega_{ve} + \omega_s = -\omega_{eg} + \omega_p$, that the third Lorentzian factor is the negative complex conjugate of the second one, so that the line shape can be approximated as follows:

$$S_{Raman} = -i \frac{\rho_{gg}^{(0)}}{\omega_{vg} - (\omega_p - \omega_s) - i\Gamma_{vg}} |\alpha_R|^2 + c.c. = \frac{2|\alpha_R|^2 \rho_{gg}^{(0)} \Gamma_{vg}}{(\omega_{vg} - \omega_p + \omega_s)^2 + \Gamma_{vg}^2} \quad (10)$$

with the Raman polarisability

$$\alpha_{Raman} = \frac{(\vec{\epsilon}_L \cdot \vec{\mu}_{ge})(\vec{\epsilon}_S^* \cdot \vec{\mu}_{ev})}{\omega_{eg} - \omega_p - i\Gamma_{eg}} \quad (11)$$

The CARS line shape can be expressed in the Raman line shape when all involved lasers and analyzers are polarized in the same direction: $\vec{\epsilon}_p = \vec{\epsilon}_s = \vec{\epsilon}_{AS}$. With this condition one obtains:

$$S_{CARS} = \frac{\rho_{gg}^{(0)} |\alpha_R|^2 Q^2}{2\Gamma_{vg}} S_R = \frac{(\omega_{vg} - \omega_p + \omega_s)^2 + \Gamma_{vg}^2}{4\Gamma_{vg}^2} Q^2 S_R^2 \quad (12)$$

with $Q = (\omega_{eg} - \omega_p - i\Gamma_{eg}) / (\omega_{eg} - \omega_{AS} - i\Gamma_{eg})$. When the lowest electronic excitation lies far beyond a single photon transition from the ground state (i.e. for $\omega_{eg} \gg \omega_p, \omega_{AS}$) one has $Q \rightarrow 1$. Thus when measuring CARS spectra with the polarisation of all fields (ω_p , ω_s and ω_{AS}) parallel, the data can be compared directly to that obtained with spontaneous Raman scattering if the scattered light is detected parallel to that of the excitation.

Signal-to-noise. In the last part of this section we wish to compare the fundamental limitations on signal-to-noise ratios for two different approaches to CARS measurements: the ‘total signal approach’ (denoted by S_{CARS}^{total}) and the ‘resonant-only signal approach’ (denoted by $S_{CARS}^{res-only}$). In S_{CARS}^{total} all photons emitted by the third-order polarisation in the forward direction are measured. As already shown in equation (7) the signal strength in this case can - for low solute (propanol) concentration - be written as:

$$S_{CARS}^{total} \approx (N_w \chi_{NR,w})^2 + 2N_w N_{prop} \chi_{NR,w} \text{Re}\{\chi_{R,prop}\} \quad (13)$$

Since - still in the case of low propanol concentration - the first (or background) term in eq 13 is much larger than the second (or signal) term, the signal-to-noise ratio in S_{CARS}^{total} reads, for a total measuring time Δt and a detector dark count rate (including dark current, read-out noise, etc.) I_D :

$$SNR_{CARS}^{total} \approx \frac{2N_w N_{prop} \chi_{NR,w} \operatorname{Re}\{\chi_{R,prop}\} \Delta t}{\sqrt{(I_D \Delta t)^2 + (N_w \chi_{NR,w})^2 \Delta t}} \quad (14)$$

Alternatively, various techniques are available (see also the discussion below) to isolate the resonant contribution to the signal only:

$$S_{CARS}^{res-only} = |N_{prop} \chi_{R,prop}|^2 \quad (15)$$

In this case, the signal-to-noise ratio is determined by the Poisson noise of the signal and the detector dark current:

$$SNR_{CARS}^{res-only} = \frac{|N_{prop} \chi_{R,prop}|^2 \Delta t}{\sqrt{(I_D \Delta t)^2 + |N_{prop} \chi_{R,prop}|^2 \Delta t}} \quad (16)$$

In order to compare the two ratios quantitatively, we assume that the real and imaginary parts of the resonant susceptibility are of equal magnitude (which is found often in practice - data not shown). In S_{CARS}^{total} the laser powers and measurement time Δt are chosen such as to nearly saturate the CCD camera: $(N_w \chi_{NR,w})^2 = 300.000$ counts/s. In this case, the CCD noise sources (dark current, read-out noise, etc.) are negligible, and the signal-to-noise ratio may be approximated by the expression $SNR_{CARS}^{total} \approx \sqrt{2} \cdot N_{prop} |\chi_{R,prop}| \sqrt{\Delta t}$. Thus, the detected signal depends linearly on the propanol concentration and is fundamentally limited only by Poisson noise: longer exposure times progressively increase the detection sensitivity.

For $S_{CARS}^{res-only}$ on the other hand, the signal level drops quadratically with the propanol concentration and the detection sensitivity is fundamentally limited by the detector dark current. It is not straightforward to compare the two approaches directly, since the effectively generated signal depends on various factors, such as chosen pulse duration of the lasers and linewidth of the vibrational mode. However, whereas the multiplex CARS approach with total signal detection may continue to increase its detection sensitivity by increasing the acquisition time, the 'resonant-only signal approach' is limited fundamentally by detector dark current.

3. MATERIALS AND METHODS

The experimental set-up has been described in detail elsewhere [6]. Briefly, multiplex CARS experiments were performed using two tunable mode-locked Ti:sapphire lasers, pumped by a Nd:YVO4 laser. The pump laser operates in picosecond mode, with pulses of 10 ps (bandwidth ~ 1 cm⁻¹ fwhm), centered around 710 nm. The Stokes pulses have a duration of 80 fs, corresponding to a bandwidth of ~ 180 cm⁻¹ fwhm and are centered around 900 nm for excitation in the C-H stretch vibrational region (2800-3100 cm⁻¹). Typically, the average powers of the pump and Stokes lasers are 200 mW and 15-25 mW respectively. The pump and Stokes pulses are overlapped collinearly on a 710-nm Notch filter (Kaiser Optical Systems). In the propanol dilution experiments the laser beams are focused into a cuvet with 50 mm focal length achromat. For the lipid bilayer experiments, the lasers are focused with a microscope objective (1.25 NA, 63 \times , oil immersion) onto the sample. The CARS signal is collected in the forward direction, through a 710-nm short wave pass filter (Omega). Spectra are obtained by

dispersing the light through a spectrograph (Oriel MS 257) onto a CCD camera (Andor V420-OE). The spectral resolution of $\sim 5 \text{ cm}^{-1}$ is determined by the resolving power of the spectrograph.

For sensitive detection of the CARS signal at low solute concentration, it is essential to measure accurately the spectral shape of the non-resonant contribution, which is determined by the Stokes spectral profile. In the propanol dilution experiments we therefore accumulate the ratio between alternately measured CARS signals of two cuvettes, one containing pure water and the other containing the water dissolved propanol sample. The individual acquisition time of a single CARS spectrum is 20 ms, and between 4 and 2000 accumulations are used over the range of 30 to 0.03 volume % propanol in water. In the lipid bilayer experiments, the sample and reference signal are derived from acquisitions taken at an axial position of the laser focus centred on the bilayer and within the glass respectively.

Spontaneous Raman scattering spectra were measured with a Raman microscope (Renishaw RM1000, spectral resolution: $\sim 5 \text{ cm}^{-1}$) with a 6 mW HeNe laser. The plane of polarization of the exciting radiation was parallel to the direction of observation.

2-Propanol (Merck, purity > 99.7%) was used without further purification. Lipids - 1,2-dipalmitoyl-sn-glycero-3-phosphocholine (DPPC, 16:0), 1,2-dipalmitoyl-D62-sn-glycero-3-phosphocholine (d62-DPPC, 16:0) and 1,2-dioleoyl-sn-glycero-3-phosphocholine (DOPC; 18:1, 9-cis) - were obtained from Avanti Polar lipids and were checked for purity using thin layer chromatography. Supported planar bilayers (SPB) were prepared using the Langmuir-Blodgett technique (see [12] for details). The bilayer preparation procedure was checked by adding 1 mol% 1,1'-dioctadecyl-3,3,3',3'-tetramethylindocarbocyanine perchlorate (diIC18, Molecular Probes) to the lipid. Using a fluorescence microscope, the homogeneity of the SPBs was found to be satisfactory.

4. EXPERIMENTAL RESULTS

Figure 1 shows the spontaneous Raman signal and multiplex CARS signal from a 10% by volume dilution of 2-propanol in water. The vibrational spectrum is dominated by four resonant features from CH-stretch vibrations of propanol, on a flank of the 3200 cm^{-1} vibrational band of water. The fit of the spontaneous Raman data (figure 1a) uses a sum of five Lorentzian contributions. The thus derived line widths, positions and amplitudes can then be used directly to describe the multiplex CARS signal (see theoretical section above). These parameters are used for the solid line in figure 1b. Note the excellent agreement between Raman and multiplex CARS data.

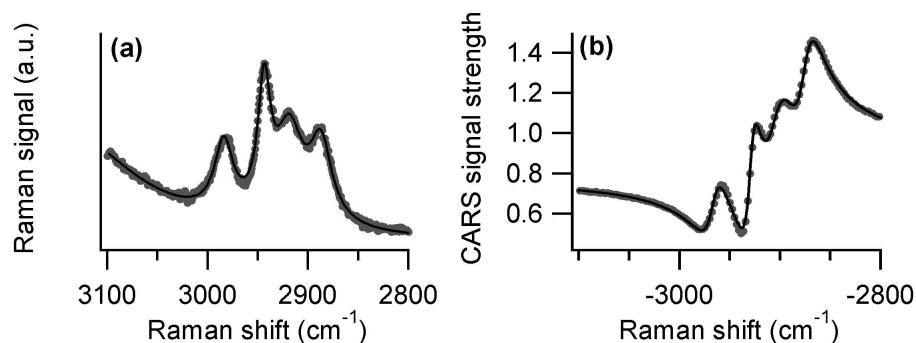


Figure 1. (a) Spontaneous Raman and (b) multiplex CARS spectra of 10 volume % dilution of 2-propanol in water. Dots: experimental data points. Solid line: theoretical fit. The spectral parameters determined for the spontaneous Raman spectrum are used directly to describe the multiplex CARS data. Acquisition time (a) Raman: 300 s; (b) CARS: 80 ms.

Next, a dilution series of propanol in water (between 0.03 and 30 volume %) was measured in multiplex CARS. The experimental data were fitted with only two free parameters: the amplitude of the 2943 cm^{-1} resonant vibrational mode and the magnitude of the non-resonant background. Examples of these measurements are shown in figure 2. There is excellent agreement between theory and the experimental data. It should be noted - demonstrating the sensitivity of this approach to the actual shape of the spectrum - that it is crucial to include the moderate resonant contribution from water in the theoretical description of the data. For the highest propanol concentration (30%) the fitting becomes less accurate because of vibrational spectral changes due to reduced hydrogen bonding. (For pure propanol, the 2976 cm^{-1} feature significantly decreases in amplitude relative to the 2943 cm^{-1} vibrational mode in comparison to diluted samples.)

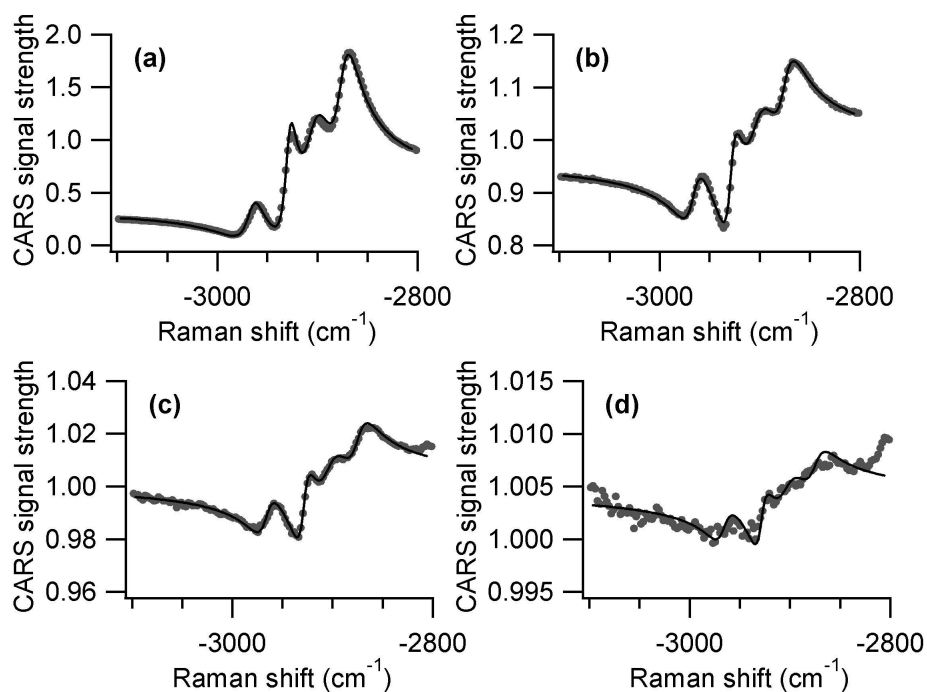


Figure 2. Multiplex CARS spectra at different dilutions of 2-propanol in water: (a) 30, (b) 3, (c) 0.3 and (d) 0.03 volume %. Dots: experimental data points. Solid line: theoretical fit. The only free parameters used in the fit of the experimental data are the amplitude of the 2943 cm^{-1} vibrational mode and the magnitude of the non-resonant contribution. Acquisition times: (a) 80 ms; (b) 200 ms; (c) 4 s; (d) 40 s.

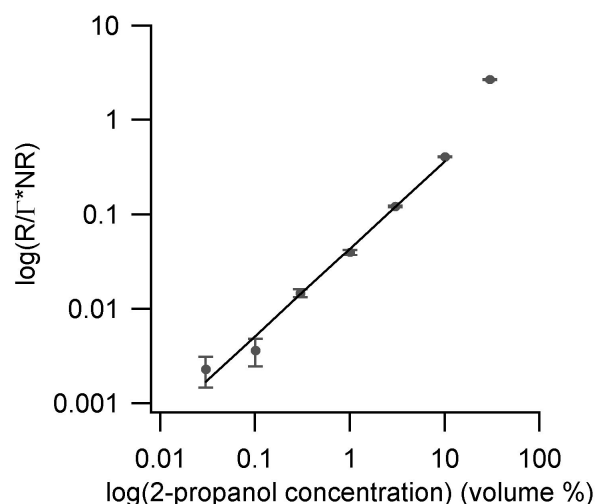


Figure 3. Multiplex CARS signal strength of the 2943 cm^{-1} vibrational mode as a function of propanol concentration in water. The 30% concentration deviates from the linear dependence through a combination of an increased importance of the resonant term in equation (6), as well as a change in shape of the spectrum due to reduced hydrogen bonding.

An absolute signal strength can be derived from the data, expressed as the ratio of the amplitude of the resonant contribution over the product of its linewidth and the magnitude of the non-resonant contribution: $R/\Gamma \cdot NR$. This value is shown as a function of propanol concentration for the 2943 cm^{-1} vibrational mode in figure 3. The expected linear behaviour at low propanol concentrations is clearly demonstrated by the experimental data.

As a final demonstration of the sensitivity of the multiplex CARS technique, figure 4 shows the multiplex CARS signal from a *single* lipid mono- and bilayer deposited on glass. Discrimination of a single lipid mono-layer was achieved by preparing a bilayer of which one leaflet contained DOPC, whereas the other contained fully deuterated d62-DPPC, and measuring the CD-stretch region around 2100 cm^{-1} . Also shown in figure 4 is multiplex CARS signal from a single lipid bilayer consisting only of fully deuterated d62-DPPC. Importantly, the signal strength provides an absolute measure of the lipid density within the focal volume of the laser beams. This is shown by the factor of two difference in signal strength between the two measurements. Independently we have determined that the signal-to-noise ratio in this case is solely determined by shot-noise. Even for an acquisition time of only 20 ms, the signal-to-noise ratio is sufficient to determine the order parameter of the acyl chains from the experimental data.

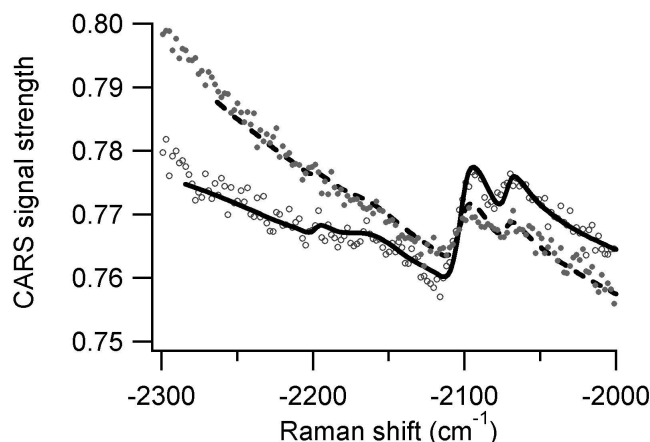


Figure 4. Multiplex CARS signal from a single lipid mono- (dotted curve, closed symbols) and bilayer (straight curve and open symbols). Dots are the experimental data points, solid lines represent theoretical fits to the data. (See text for further details.)

5. DISCUSSION

This paper demonstrates the shot-noise limited sensitivity of multiplex CARS microscopy/spectroscopy. This technique actually uses - rather than suppresses - the non-resonant background to boost the signal from the resonant vibrational mode of interest in a heterodyne fashion. This approach is different from various other approaches that attempt to increase the sensitivity by suppressing the non-resonant background either through specific polarized excitation and detection [13], epi-detection [14], time-resolved measurements [8] or through combined polarization and phase control [15].

Obtaining accurate CARS spectra is crucial when attempting to determine the chemical identity of the measured species or the physical state of the sample. The conventional CARS approach, using both a narrow band *pump* and *Stokes* laser, generally cannot provide spectra of sufficient accuracy. The signal-to-noise of the acquired spectrum in this case suffers from all laser related fluctuations (power, jitter, etc.). Also, tuning and acquisition with sufficient spectral resolution is often time consuming.

In contrast, multiplex CARS provides high quality spectra of which the signal-to-noise is limited by shot-noise only. When applied to low solute concentrations it is important to measure accurately the shape of non-resonant background. This can be done either within the same sample (as in microscopic applications) or using a reference cuvet. The latter case shows great potential for high sensitivity CARS spectroscopy. Various experimental schemes can be considered to obtain the CARS signal from both the sample and the reference, either sequentially (as shown here) or simultaneously. It should be noted, that in the first case one becomes sensitive to low frequency spectral changes of the laser, whereas in the second case the available power per acquisition is significantly reduced.

ACKNOWLEDGEMENT

This work was financially supported, in part, by the Foundation for Fundamental Research on Matter (FOM) and by Aard- en Levenswetenschappen (ALW), the Netherlands under grant no. 94RG02 and 805.47.040.

REFERENCES

1. G. J. Puppels, et al., "Studying single living cells and chromosomes by confocal Raman microspectroscopy," *Nature* **347**, 301-303 (1990).
2. A. Zumbusch, et al., "Three dimensional vibrational imaging by coherent anti-Stokes Raman scattering," *Phys. Rev. Lett.* **82**, 4142-4145 (1999).
3. M. Müller, et al., "CARS microscopy with folded BoxCARS phasematching," *J. Microsc.* **197**, 150-158 (2000).
4. A. Volkmer, et al., "Vibrational imaging with high sensitivity via epidetected coherent anti-Stokes Raman scattering microscopy," *Phys. Rev. Lett.* **87**, 23901-1/4 (2001).
5. J. Cheng, et al., "Polarization coherent anti-Stokes Raman scattering microscopy," *Opt. Lett.* **26**, 1341-1343 (2001).
6. M. Müller, et al., "Imaging the thermodynamic state of lipid membranes with multiplex CARS microscopy," *J. Phys. Chem. B* **106**, 3715-3723 (2002).
7. G. W. H. Wurpel, et al., "Chemical specificity in 3D imaging with multiplex CARS microscopy," *Opt. Lett.* **27**, 1093-1095 (2002).
8. A. Volkmer, et al., "Time-resolved coherent anti-Stokes Raman scattering microscopy: imaging based on Raman free induction decay," *Appl. Phys. Lett.* **80**, 1505-1507 (2002).
9. J. Cheng, et al., "Coherent anti-Stokes Raman scattering correlation spectroscopy: Probing dynamical processes with chemical specificity," *J. Phys. Chem. A* **106**, 8561-8568 (2002).
10. Y. Prior, "A complete expression for the third-order susceptibility ($\chi^{(3)}$) - Perturbative and diagrammatic approaches," *IEEE J. Quant. Electr.* **20**, 37-42 (1984).
11. S. Mukamel, in *Principles of nonlinear optical spectroscopy* (Oxford University Press, Oxford, 1995).
12. G. W. H. Wurpel, et al., "Direct measurement of chain order in single lipid mono- and bilayers with multiplex CARS," *J. Phys. Chem. B* (2003).
13. S. A. Akhmanov, et al., "Polarization active Raman spectroscopy and coherent Raman elipsometry," *Sov. Phys. JETP* **47**, 667-678 (1978).
14. J. Cheng, et al., "An epi-detected coherent anti-Stokes Raman scattering (E-CARS) microscope with high spectral resolution and high sensitivity," *J. Phys. Chem. B* **105**, 1277-1280 (2001).
15. D. Oron, et al., "Femtosecond Phase-and-Polarization Control for Background-Free Coherent Anti-Stokes Raman Spectroscopy," *Phys. Rev. Lett.* **90**, 213902 (2003).